

# Experimental Study of Hall Effect on a Formation Process of an FRC by Counter-Helicity Spheromak Merging in TS-4<sup>\*</sup>)

Yasuhiro KAMINOU, Michiaki INOMOTO and Yasushi ONO

*Graduate School of Engineering, The University of Tokyo, Tokyo 113-8656, Japan*

(Received 29 November 2015 / Accepted 2 March 2016)

Hall effect on counter-helicity spheromak merging is experimentally investigated in a low- $S^*$  region, where  $S^*$  is the ratio of plasma minor radius to ion skin depth. Direct measurement of magnetic field, ion flow, electron density revealed that Hall effect affect not only merging reconnection phase but also relaxation phase through formation of ion flow and current density profiles. Hall effect breaks the symmetry of the “case-O” and “case-I” counter-helicity spheromak merging, which are defined by combinations of poloidal flux and toroidal flux of initial spheromaks. Formation of toroidal current profile and radial outflow pattern are different in case-O and case-I during merging process, and that results in great difference of profiles of electron density after merging.

© 2016 The Japan Society of Plasma Science and Nuclear Fusion Research

Keywords: magnetic reconnection, field-reversed configuration, hall effect, plasma merging, spheromak, high-beta

DOI: 10.1585/pfr.11.2401052

## 1. Introduction

A field-reversed configuration (FRC) [1] is an attractive configuration because of its high-beta. High-beta magnetic confinement is important for economical fusion reactor, and the simply-connected structure of an FRC enables to make a fusion reactor simple. The counter-helicity spheromak merging (CHSM) [2–4] is one of the method of creating an FRC, and it has an advantage that it can easily generate a large-flux FRC, compared with Field-Reversed Theta Pinch (FRTP) method. Direct formation of an FRC by FRTP need high-voltage fast capacitor bank and fast formation time, while CHSM need middle-voltage capacitor bank because a spheromak can be made slowly by a magnetized coaxial plasma gun or a flux-core, and slow formation enables a plasma to get large poloidal magnetic flux. And it also contains some complicated phenomenon in the merging process, such as magnetic reconnection [5] and relaxation. In both phenomenon, it is considered or proved that Hall effect or the kinetic effect plays some important roles [6–9]. In magnetic reconnection, it is known that Hall effect enhances reconnection rate, that is revealed by Particle-in-Cell (PIC) simulations [10] or experiments [5]. And in theoretical predictions, high beta plasma is generated with strong ion flow by relaxation process [11]. Some experiments suggest that MHD is not related to the stability of an FRC [3, 8], and ion flow through magnetic reconnection enhances the stability of an FRC [12]. However, in CHSM, the relationship between merging reconnection process and global structures of the formed FRC have not been investigated, especially in a

condition that the Hall effect is strong. The index of Hall effect is  $S^*$ , which is defined as the ratio between plasma characteristic length and ion skin depth, and Hall effect is strong in low  $S^*$  plasma. Especially, it has not been investigated the formation process and difference between two cases of CHSM, where the difference can be strong in a low- $S^*$  condition. The two cases are called as “case-O” and “case-I”, which are defined by combinations of a polarity of poloidal flux and toroidal flux [6]. Figure 1 shows schematics of CHSM method and two cases of CHSM. In CHSM, two spheromaks with opposite toroidal magnetic flux merge together, and then an FRC with no toroidal magnetic flux is generated. In this method, there exist two patterns of CHSM with the combinations of a polarity of

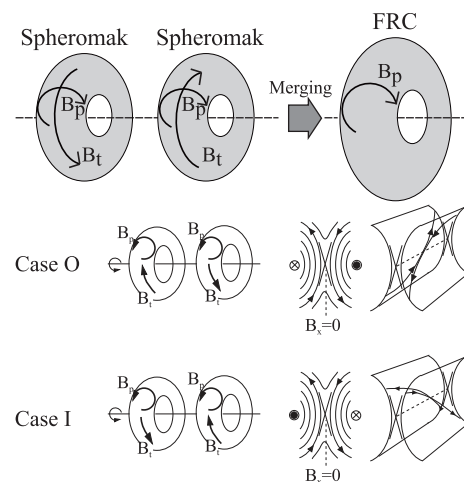


Fig. 1 A schematic of counter-helicity spheromak merging method and an illustration of “case-O” and “case-I” counter-helicity merging [14].

author's e-mail: kaminou@ts.t.u-tokyo.ac.jp

<sup>\*</sup>) This article is based on the presentation at the 25th International Toki Conference (ITC25).

poloidal flux and toroidal flux. One is called “case-O”, in which the plasma current is positive (poloidal magnetic flux is positive) and toroidal flux is positive at the +Z side, and toroidal flux is negative at the -Z side. The other is called “case-I”, in which the plasma current is positive and toroidal flux is negative at the +Z side, and toroidal flux is positive at the -Z side. The reconnection plane is tilted to toroidal direction because both poloidal field and toroidal field reconnect, and the reconnection electric field and reconnection current have both toroidal and radial components. In the reconnection current sheet,  $E_t$  and  $j_t$  are negative ( $E_t < 0$ ,  $j_t < 0$ ) in both case-O and case-I, while  $E_r$  and  $j_r$  are negative ( $E_r < 0$ ,  $j_r < 0$ ) in case-O and positive ( $E_r > 0$ ,  $j_r > 0$ ) in case-I [13]. In plasma merging, the difference of the tilting direction of the reconnection plane between case-O and case-I breaks symmetry between the two cases because the merging plasma are tori [6]. The toroidal effect couples with Hall effect during merging process and that can affect global structure of a merging-formed FRC. However, the Hall effect on a formed FRC has not been investigated, while only reconnection process of CHSM has been studied in previous works [6, 13, 14]. In this paper, we investigated influences of Hall effect during merging on the formed FRC after merging, especially a relationship between merging process and formation of current and electron density profiles.

## 2. Experimental Setup

Figure 2 shows a schematic of TS-4 plasma merging

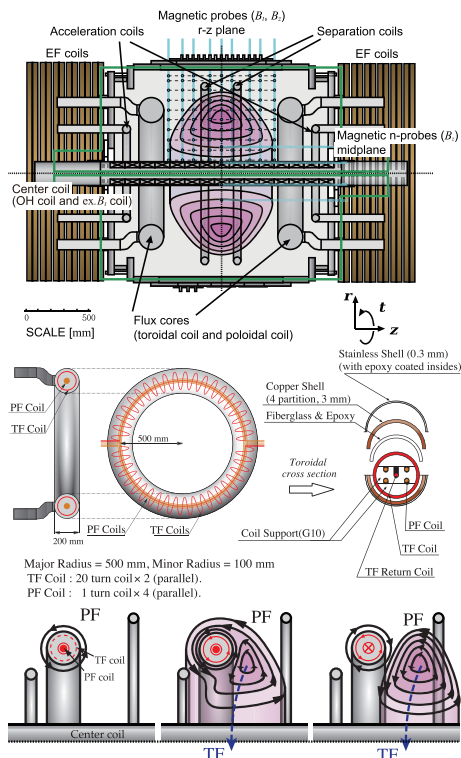


Fig. 2 Schematics of a flux core and formation process of a spheromak by the flux core.

device [4] and flux cores. Two flux cores are installed at each side of the vacuum vessel. They contain both poloidal coils (PF coils) and toroidal coils (TF coils), and they create spheromaks around them by swinging both PF coils and TF coils. After the PF coil currents are reversed, the two spheromaks are cut off by the flux cores, and pushed toward the center of the vacuum vessel ( $Z = 0$  m). Then, the two plasma merge together by magnetic reconnection, and a single plasma is formed. The typical parameters are as follows: poloidal magnetic field  $B_{\text{pol}} \sim 20$  mT, and electron density  $n_e = 10^{20} \sim 10^{21} \text{ m}^{-3}$ , plasma current  $I_p \sim 30$  kA. The electron temperature is about  $5 \sim 10$  eV, and the ion ramor radius ( $r_L$ ) is  $r_L \sim 10$  cm at the separatrix. In this condition, ions are weakly magnetized ( $s = a/r_L \sim 2$ ,  $a$  is the plasma minor radius.) and the Hall effect is strong ( $S^* = a/l_i \sim 2$ ,  $l_i$  is the ion skin depth).

For measurement of two-dimensional profiles of magnetic field and current profile, 2D magnetic probe arrays were used. Magnetic field to  $z$  direction ( $B_z$ ) were firstly measured in various  $R$  and  $Z$  positions, and then poloidal magnetic flux was estimated by the integration of  $B_z(r, z)$  with the assumption of axisymmetry. Finally, radial magnetic field ( $B_r$ ) was got from equation (2).

$$\Psi(r, z) = \int_{r_{\min}}^r B_z(r, z) \cdot 2\pi r dr, \quad (1)$$

$$B_r = -\frac{1}{2\pi r} \frac{\partial \Psi}{\partial z}. \quad (2)$$

For measurement of ion flow and electron density, A Mach probe and a Langmuir probe are installed at the mid-plane ( $Z = 0$  m). A Mach probe can measure ion mach number ( $M_i = v_i/c_s$ ,  $c_s = \sqrt{\frac{\gamma(T_i + T_e)}{m_i}}$ ) by comparing ion saturation current at upstream electrode ( $j_{\text{up}}$ ) and downstream electrode ( $j_{\text{down}}$ ).

$$\frac{j_{\text{up}}}{j_{\text{down}}} = \exp(KM_i), \quad (3)$$

$K$  is a constant parameter, and we adopt  $K = 2.0$  for weakly magnetized condition, which have been got by SSX experiment [15]. In this experiment,  $T_i = T_e$  is assumed because little electron or ion heating occurs in the condition that radiation loss is large and ions do not have gyro-motion with weak magnetic field.  $T_e$  is measured by a Langmuir probe [14]. The Langmuir probe and the Mach probe can be swept shot-by-shot, and radial profiles of these quantities are got by assuming reproducibility.

## 3. Results & Discussions

### 3.1 Global structure of magnetic fields

We report relation between current profile formation and the Hall effect during merging process in this section. Figures 3, 4 show poloidal flux contour (poloidal magnetic field lines) and toroidal magnetic field in case-O/I CHSM measured by 2D magnetic probe arrays. In Fig. 3 (case-O), the toroidal flux at +Z side is positive, and the toroidal flux at -Z side is negative. In Fig. 4 (case-I), the toroidal flux

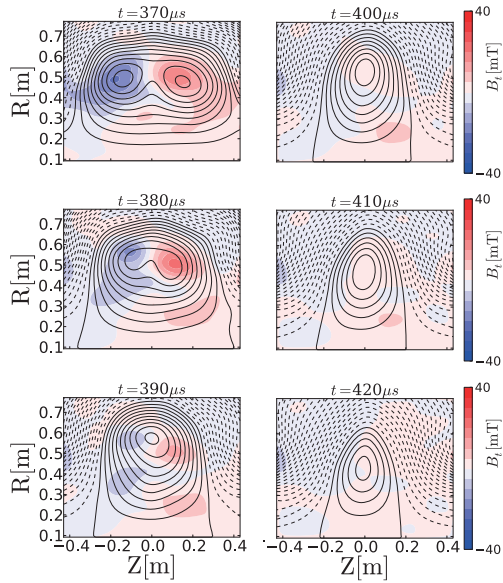


Fig. 3 Poloidal flux contour (line) with toroidal magnetic field (colored) in Case-O.

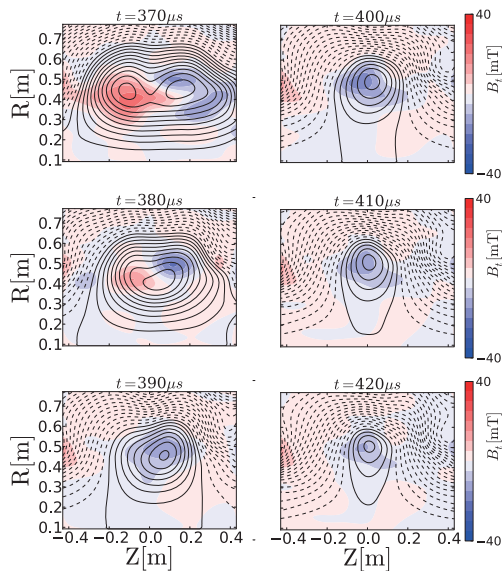


Fig. 4 Poloidal flux contour (line) with toroidal magnetic field (colored) in Case-I.

at  $+Z$  side is negative, and the toroidal flux at  $-Z$  side is positive. In both figures, toroidal plasma currents are positive. Figure 5 shows time evolutions of X-point (during merging) and O-point of the formed FRCs (after merging), and the separatrix radius. In case-O, the X-point moves outward in the radial direction, and in case-I, it moves inward during merging. The direction of the movement of the X-point is same as the radial component of the reconnection current. In case-O, radial current in the current sheet is negative because the spheromak at the  $+Z$  side has positive toroidal magnetic field and the spheromak at the  $-Z$  side has negative toroidal magnetic field. And the di-

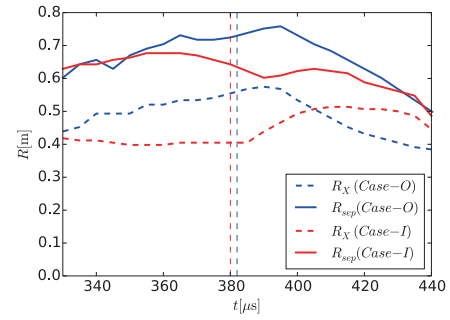


Fig. 5 Time evolutions of the X-point/O-point radius ( $R_X$ ) and the separatrix radius ( $R_{sep}$ ) in case-O (blue) and case-I (red). The vertical lines show merging completion time of case-O (blue) and case-I (red).

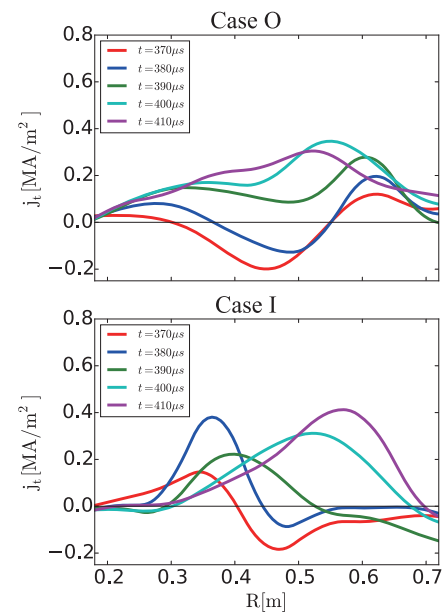


Fig. 6 Radial profiles of toroidal current ( $j_t$ ) in case-O (top) and case-I (bottom).

rection of the X-point movement is outward. On the other hand, in case-I, radial current in the current sheet is positive because the spheromak at the  $+Z$  side has negative toroidal magnetic field and the spheromak at the  $-Z$  side has positive toroidal magnetic field. And the direction of the X-point movement is inward. Coupled with previous studies [16, 17] that Hall reconnection moves the X-point in the same direction as the reconnection current, it is assumed that the X-point moves both toroidal (negative) and radial (negative in case-O and positive in case-I) direction in this experiment. These results are consistent with previous experiment in MRX [6]. By the motion of the X-point, it is found that the toroidal current profiles during and after merging are different between case-O and case-I. Figure 6 shows the profiles of toroidal current density ( $j_t$ ) at  $Z = 0$  m in case-O and case-I, which are measured by 2D magnetic probe arrays. The direction of plasma

current of the initial spheromaks are toroidally positive ( $j_t > 0$ ). These are same characteristics and difference between case-O and case-I. The same characteristic is current sheet position during reconnection ( $t = 370 \mu\text{s}$ ). Current sheet peak is located on  $R \sim 0.45 \text{ m}$  and the X-point is  $R \sim 0.5 \text{ m}$  at  $t = 370 \mu\text{s}$  in case-O, while the current sheet peak is located on  $R \sim 0.45 \text{ m}$  and the X-point is  $R \sim 0.4 \text{ m}$  at  $t = 370 \mu\text{s}$  in case-I. Thus, the same characteristic is that the current sheet peak shifts to the opposite direction to the motion of the X-point. However, current profile after merging has difference between case-O and case-I. Hollow current profile is formed just after merging completion ( $t = 390 \mu\text{s}$ ) in case-O. After that, the current profile relaxes to broad profile ( $t = 410 \mu\text{s}$ ). On the other hand, in case-I, the current profile after merging is sharply peaked ( $t \geq 390 \mu\text{s}$ ). During merging, positive current arises at the inboard side of the X-point, and this is caused by the compression of the poloidal magnetic field ( $B_z$ ) by the inward displacement of the X-point ( $t \leq 380 \mu\text{s}$ ). The inward displacement of the X-point enhances the magnetic pressure of the poloidal magnetic field in case-I, and then the strong gradient of poloidal magnetic pressure makes positive toroidal current at the inboard side of the X-point (during merging) or O-point (after merging). At the outboard side, magnetic pressure becomes weak, and positive toroidal current is suppressed. In case-O, compression of poloidal magnetic pressure is not strong because the direction of the X-point motion is outward and the outboard side. Instead, the X-point motion makes the separatrix larger. Thus, it is concluded that the hollow current profile in case-O and the peaked current profile in case-I after merging is derived from the Hall effect in the merging process.

### 3.2 Flow and density profiles

To investigate influences of Hall effect on flow formation during merging and density profiles after merging, we measured radial profiles of radial ion flow, electron density, and electron temperature by a Mach probe and a Langmuir probe (a triple probe) at  $Z = 0 \text{ m}$ . We found that ion flow caused by reconnection is strongly biased to one side, and the direction depends on the polarity of the reconnecting toroidal magnetic flux. Figure 7 shows radial profiles of radial ion flow at  $Z = 0$ . In case-O, radial flow is strong in negative direction. The flow is strongly negative at the inboard side of the X-point ( $R < 0.5 \text{ m}$ ), and weakly positive at the outboard side of the X-point. On the other hand, in case-I, radial flow is strong in positive direction. The flow is weakly negative at the inboard side of the X-point ( $R < 0.4 \text{ m}$ ), and strongly positive at the outboard side of the X-point. Thus, ion acceleration was observed during the merging process, and this acceleration seems to be strongly related with Lorentz force ( $j \times B$ ), which is modified by the Hall effect. Figure 8 shows the time evolution of Lorentz force calculated by radial profiles of toroidal current and poloidal magnetic field from equation (4).

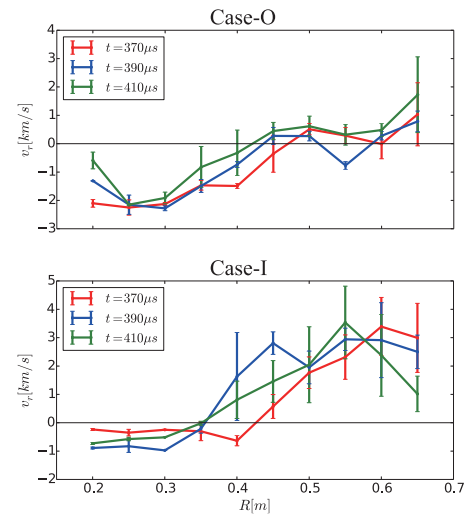


Fig. 7 Radial flow profiles at  $Z = 0$  in case-O (top) and case-I (bottom).

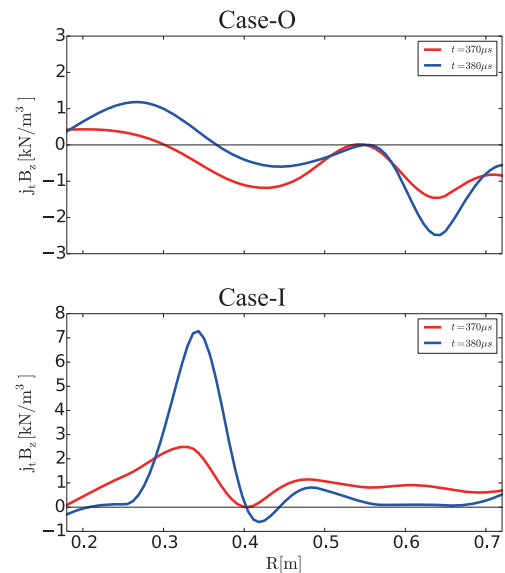


Fig. 8 Radial component of  $j \times B$  force ( $j_t B_z$ ) profiles in case-O (top) and case-I (bottom).

$$(j \times B)_r = j_t B_z. \quad (4)$$

During merging ( $t \leq 380 \mu\text{s}$ ), the sign of  $j_t B_z$  is negative in almost all region in case-O. This is because the magnetic field ( $B_z$ ) is compressed in the outboard side of the X-point by the displacement of the X-point which is caused by the Hall effect, and then the compressed poloidal magnetic field makes positive toroidal current. At the inboard side of the X-point, the displacement of the X-point enhances magnetic tension and negative toroidal current. Therefore, the  $j_t B_z$  force is negative and reconnection outflow is mainly accelerated to inward. The negatively biased radial ion outflow pattern in case-O seemed to be caused in this way. On the other hand, in case-I, the  $j_t B_z$  force is positive in almost all region during reconnection. This

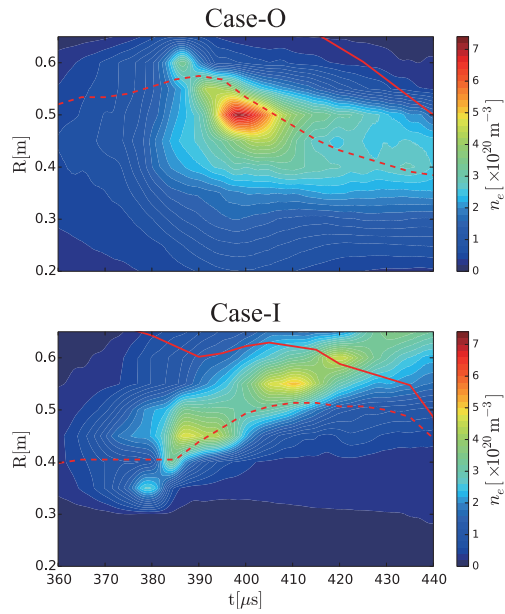


Fig. 9 Time evolution and radial profile of electron density in case-O/I. The dashed line shows X-point (during merging)/O-point (after merging) radius, and the solid line shows separatrix radius.

is because the magnetic field ( $B_z$ ) is compressed in the inboard side of the X-point by the inward displacement of the X-point which is caused by the Hall effect, and then the compressed poloidal magnetic field makes strong positive toroidal current. At the outboard side of the X-point, the displacement of the X-point enhances magnetic tension and negative toroidal current. Therefore, the  $j_t B_z$  force is positive and reconnection outflow is mainly accelerated outward. The positively biased radial ion outflow pattern in case-I seemed to be caused in this way. Electron density profile after merging completion also has strong relationship with the Hall effect. Figure 9 shows time evolution and radial profiles of electron density at  $Z = 0$  m in case-O and case-I. The solid red line shows a separatrix radius of the plasma at  $Z = 0$  m, and the dashed red line shows the X-point of the magnetic reconnection (during merging) and O-point of the formed FRC (after merging). In case-O, the electron density peak moves inward, and it is trapped inside the separatrix. On the other hand, the electron density peak moves outward and it is not trapped inside the separatrix. It is assumed that the bulk ions moves with the radial ion flow generated during the merging process, and large inertia of the ions enabled to leave the flow pattern after merging. Thus, these results demonstrated that the Hall effect during merging affects not only recon-

tion process but also profiles of density profile and global magnetic field profile of a merging-formed FRC.

## 4. Summary

Influences on formation of flow, current profile, and electron density profile by the Hall effect in the formation process of a merging-formed FRC in a low- $S^*$  condition was investigated through comparing two cases of counter-helicity spheromak merging. In the TS-4 experiment, it was observed that the X-point in case-O merging moves outward, and the X-point in case-I merging moves inward. The X-point movement generates compression of poloidal magnetic pressure, and then the Lorentz force by this effect produces strong bias of the radial outflow, which affects electron density profile after merging completion. It was also found that hollow current profile is formed in case-O, and peaked current profile is formed in case-I at merging completion period. It is concluded that the current profiles and flow patterns formed by Hall reconnection in merging phase has large influence on global electron density profile of formed FRCs after merging completion.

## Acknowledgement

This work was supported by JSPS Fellows (27-8028), JSPS A3 Foresight Program “Innovative Tokamak Plasma Startup and Current Drive in Spherical Torus”, and the NIFS Collaboration Research program (NIFS14KNWP004).

- [1] L.C. Steinhauer, *Phys. Plasmas* **18**, 070501 (2011).
- [2] M. Yamada *et al.*, *Phys. Rev. Lett.* **65**, 721 (1990).
- [3] S.P. Gerhardt *et al.*, *Phys. Rev. Lett.* **99**, 245003 (2007).
- [4] T. Ii *et al.*, *Nucl. Fusion* **53**, 073002 (2013).
- [5] M. Yamada *et al.*, *Rev. Mod. Phys.* **82**, 603 (2010).
- [6] M. Inomoto *et al.*, *Phys. Rev. Lett.* **97**, 135002 (2006).
- [7] E. Kawamori and Y. Ono, *Phys. Rev. Lett.* **95**, 085003 (2005).
- [8] R. Horiuchi *et al.*, *Nucl. Fusion* **39**, 2083 (1999).
- [9] H. Ohtani *et al.*, *Phys. Plasmas* **10**, 145 (2003).
- [10] R. Horiuchi and T. Sato, *Phys. Plasmas* **4**, 277 (1997).
- [11] L.C. Steinhauer and A. Ishida, *Phys. Rev. Lett.* **79**, 3423 (1997).
- [12] Y. Ono *et al.*, *Nucl. Fusion* **43**, 649 (2013).
- [13] Y. Kaminou *et al.*, *IEEJ Trans. FM.* **133**, 412 (2013) (in Japanese).
- [14] Y. Kaminou *et al.*, *IEEJ Trans. FM.* **134**, 487 (2014) (in Japanese).
- [15] X. Zhang *et al.*, *Rev. Sci. Instrum.* **82**, 033510 (2011).
- [16] D.A. Uzdenski and R.M. Kulsrud, *Phys. Plasmas* **13**, 062305 (2006).
- [17] M. Yamada *et al.*, *Phys. Plasmas* **13**, 052119 (2006).